

## Magnetic phase transitions in $\text{Co}_c\text{Mg}_{1-c}\text{Cl}_2$ and stage-2 $\text{Co}_c\text{Mg}_{1-c}\text{Cl}_2$ graphite intercalation compounds

Itsuko S. Suzuki, Chi-Jen Hsieh, Floyd Khemai, Charles R. Burr, and Masatsugu Suzuki  
*Department of Physics and Materials Research Center, State University of New York at Binghamton,  
 Binghamton, New York 13902-6000*

(Received 13 July 1992)

Pristine  $\text{Co}_c\text{Mg}_{1-c}\text{Cl}_2$  and stage-2  $\text{Co}_c\text{Mg}_{1-c}\text{Cl}_2$  graphite intercalation compounds (GICs) ( $0 \leq c \leq 1$ ) approximate site-diluted three-dimensional (3D) and two-dimensional (2D)  $XY$  spin systems, respectively. We have studied the magnetic phase transitions of these two systems by using dc and ac magnetic susceptibilities. We find that the reduced critical temperature of stage-2  $\text{Co}_c\text{Mg}_{1-c}\text{Cl}_2$  GIC is almost the same as that of  $\text{Co}_c\text{Mg}_{1-c}\text{Cl}_2$  for  $c > 0.7$ . The effect of the dimensionality on the dilution with Mg ions becomes significant below  $c \approx 0.7$ . The percolation threshold for  $\text{Co}_c\text{Mg}_{1-c}\text{Cl}_2$  is  $c_p \approx 0.36$ , close to the theoretical value (0.295) for the 2D triangular lattice with nearest-neighbor (NN) and next-nearest-neighbor (NNN) exchange interactions, and the percolation threshold for stage-2  $\text{Co}_c\text{Mg}_{1-c}\text{Cl}_2$  GIC is  $c_p \approx 0.5$ , close to the theoretical value (0.5) for the 2D triangular lattice with NN exchange interaction. We also find that the peak susceptibility of  $\text{Co}_c\text{Mg}_{1-c}\text{Cl}_2$  at the Néel temperature drastically increases with decreasing Co concentration. This phenomenon is discussed in terms of recent scaling theory.

### I. INTRODUCTION

Magnetic graphite intercalation compounds (GICs)<sup>1,2</sup> are typical examples of two-dimensional (2D) spin systems. The magnetic GICs such as  $\text{CoCl}_2$  GIC and  $\text{NiCl}_2$  GIC undergo two magnetic phase transitions at  $T_{\text{cu}}$  and  $T_{\text{cl}}$ , showing 2D spin ordering in the intermediate phase between  $T_{\text{cu}}$  and  $T_{\text{cl}}$ . Because of the 2D nature of magnetic GICs, magnetic random mixture GICs (RMGICs) such as stage-2  $\text{Co}_c\text{Ni}_{1-c}\text{Cl}_2$  GIC,<sup>3</sup> stage-2  $\text{Co}_c\text{Mn}_{1-c}\text{Cl}_2$  GIC,<sup>4</sup> and stage-2  $\text{Ni}_c\text{Mn}_{1-c}\text{Cl}_2$  GIC<sup>5</sup> are believed to provide model systems for the study of the 2D random spin systems. In these compounds, two kinds of magnetic species are randomly distributed on the triangular lattice of the intercalate layer. In stage-2  $\text{Co}_c\text{Ni}_{1-c}\text{Cl}_2$  GIC, a spin frustration effect arising from competing spin anisotropies between  $XY$  and Heisenberg occurs. In stage-2  $\text{Co}_c\text{Mn}_{1-c}\text{Cl}_2$  GIC and stage-2  $\text{Ni}_c\text{Mn}_{1-c}\text{Cl}_2$  GIC, there appears a spin frustration effect arising from the competition between ferromagnetic and antiferromagnetic intraplanar exchange interactions, leading to a spin-glass behavior.

Another type of RMGIC, that is, stage-1  $\text{Co}_c\text{Mg}_{1-c}\text{Cl}_2$  GIC, has been synthesized by Nicholls and Dresselhaus.<sup>6</sup> A mixture of powdered  $\text{CoCl}_2$  and  $\text{MgCl}_2$  was intercalated into single-crystal kish graphite and highly oriented pyrolytic graphite (HOPG). A part of the Co ions are replaced by nonmagnetic Mg ions within each intercalate layer. Nicholls and Dresselhaus<sup>6</sup> have studied the effect of dilution with nonmagnetic ions on the magnetic phase transition in these compounds by ac magnetic susceptibility measurement. Nicholls and Dresselhaus<sup>6</sup> have shown that the critical temperature  $T_c$  is extrapolated to zero at the critical concentration  $c = 0.65$ , which is larger than the theoretical percolation threshold for a 2D triangular lattice with nearest-

neighbor (NN) exchange interaction:  $c_p(\text{theory}) = 0.5$ . They have claimed that such a deviation of the critical concentration ( $c = 0.65$ ) from  $c_p = 0.5$  is due to a possible 15% random distribution of voids inside the intercalate layers.

In this paper, we have undertaken an extensive study of the magnetic and structural properties of pristine  $\text{Co}_c\text{Mg}_{1-c}\text{Cl}_2$  and stage-2  $\text{Co}_c\text{Mg}_{1-c}\text{Cl}_2$  GICs by using dc and ac magnetic susceptibility, and x-ray diffraction. The  $\text{Co}_c\text{Mg}_{1-c}\text{Cl}_2$  and stage-2  $\text{Co}_c\text{Mg}_{1-c}\text{Cl}_2$  GIC are layered compounds in which the  $\text{Co}_c\text{Mg}_{1-c}\text{Cl}_2$  layers are stacked along the  $c$  axis. The  $\text{Co}^{2+}$  and  $\text{Mg}^{2+}$  ions are randomly distributed on the triangular lattice sites within each  $\text{Co}_c\text{Mg}_{1-c}\text{Cl}_2$  layer. Since the adjacent  $\text{Co}_c\text{Mg}_{1-c}\text{Cl}_2$  layers are separated by two graphite layers in the stage-2  $\text{Co}_c\text{Mg}_{1-c}\text{Cl}_2$  GIC, the interplanar exchange interaction of stage-2  $\text{Co}_c\text{Mg}_{1-c}\text{Cl}_2$  GIC is much weaker than that of  $\text{Co}_c\text{Mg}_{1-c}\text{Cl}_2$ . Then the  $\text{Co}_c\text{Mg}_{1-c}\text{Cl}_2$  and stage-2  $\text{Co}_c\text{Mg}_{1-c}\text{Cl}_2$  GIC are expected to provide model systems of 3D and 2D site-random spin systems on the triangular lattice, respectively. The magnetic phase transition of  $\text{Co}_c\text{Mg}_{1-c}\text{Cl}_2$  has been studied by Katsumata *et al.*<sup>7</sup> by using ESR measurement. The critical temperature of  $\text{Co}_c\text{Mg}_{1-c}\text{Cl}_2$  decreases with the decrease of Co concentration and is extrapolated to zero around  $c \approx 0.3$ . They have claimed the possibility of an  $XY$  spin-glass behavior in  $\text{Co}_c\text{Mg}_{1-c}\text{Cl}_2$ , which may arise from a competition between NN ferromagnetic intraplanar exchange interaction and next-nearest-neighbor (NNN) antiferromagnetic intraplanar exchange interaction.

In spite of such interest, there has been no detailed study on the magnetic phase transitions of  $\text{Co}_c\text{Mg}_{1-c}\text{Cl}_2$  and stage-2  $\text{Co}_c\text{Mg}_{1-c}\text{Cl}_2$  GIC. Here we have synthesized stage-2  $\text{Co}_c\text{Mg}_{1-c}\text{Cl}_2$  GIC by our original method: single-crystal  $\text{Co}_c\text{Mg}_{1-c}\text{Cl}_2$  is intercalated into

single-crystal kish graphite. This method of synthesis is different from that used by Nicholls and Dresselhaus<sup>6</sup> for stage-1  $\text{Co}_c\text{Mg}_{1-c}\text{Cl}_2$  GIC. The magnetic phase diagrams (critical temperature  $T_c$  vs Co concentration) of  $\text{Co}_c\text{Mg}_{1-c}\text{Cl}_2$  and stage-2  $\text{Co}_c\text{Mg}_{1-c}\text{Cl}_2$  GIC are determined from the temperature dependence of dc and ac magnetic susceptibility, and compared with that of stage-1  $\text{Co}_c\text{Mg}_{1-c}\text{Cl}_2$  GIC. The effect of dilution with Mg ions on the magnetic phase transition is discussed in association with the dimensionality of systems.

## II. BACKGROUND

The pristine  $M\text{Cl}_2$  ( $M = \text{Co}$  and  $\text{Mg}$ ) has the hexagonal (rhombohedral)  $\text{CdCl}_2$  structure. The  $M\text{Cl}_2$  layer consists of an  $M$  layer sandwiched between upper and lower Cl layers. The  $M\text{Cl}_2$  layer forms a 2D triangular lattice with fundamental lattice vectors  $\mathbf{a}_1$  and  $\mathbf{a}_2$ , where  $|\mathbf{a}_1| = |\mathbf{a}_2| = a_0$  and the angle between  $\mathbf{a}_1$  and  $\mathbf{a}_2$  is  $120^\circ$ .<sup>8,9</sup> The in-plane lattice constant is  $a_0 = 3.544 \text{ \AA}$  for  $\text{CoCl}_2$  and  $a_0 = 3.596 \text{ \AA}$  for  $\text{MgCl}_2$ .<sup>8</sup> The  $M\text{Cl}_2$  layers are stacked along the  $c$  axis with the three-layer ( $\alpha\beta\gamma$ ) stacking sequence. The in-plane positions of  $M$  atoms in  $\beta$  and  $\gamma$  layers are related to those in the  $\alpha$  layer by the fundamental translation vectors  $\Delta$  and  $2\Delta$ , respectively, where  $\Delta = (2\mathbf{a}_1 + \mathbf{a}_2)/3$ . The lattice constant along the  $c$  axis is  $17.430 \text{ \AA}$  for  $\text{CoCl}_2$  and  $17.589 \text{ \AA}$  for  $\text{MgCl}_2$ .<sup>8</sup>

For stage-2  $\text{CoCl}_2$  GIC, the separation between the Co and Cl layers is reduced  $6 \pm 3\%$  relative to the separation in the  $\text{CoCl}_2$ . Each  $\text{CoCl}_2$  layer is structurally uncorrelated with respect to other  $\text{CoCl}_2$  layers.<sup>1</sup> The in-plane structure of the  $\text{CoCl}_2$  layer forms a triangular lattice, where the lattice constant is the same as that of  $\text{CoCl}_2$ :  $a_0 = 3.55 \text{ \AA}$ . The  $\text{CoCl}_2$  layer is incommensurate with the graphite layer, and rotated by  $30^\circ$  with respect to it. The intercalate layer is formed of small islands. Peripheral chlorine ions at the island boundary provide acceptor sites for charges transferred from the graphite layer to the intercalate layer.

The spin Hamiltonian of  $\text{Co}^{2+}$  in  $\text{CoCl}_2$ <sup>10,11</sup> and stage-2  $\text{CoCl}_2$  GIC<sup>12,13</sup> can be written as

$$H = -2J \sum_{\langle i,j \rangle} \mathbf{S}_i \cdot \mathbf{S}_j + 2J_A \sum_{\langle i,j \rangle} \mathbf{S}_i \cdot \mathbf{S}_j + 2J' \sum_{\langle i,m \rangle} \mathbf{S}_i \cdot \mathbf{S}_m, \quad (1)$$

where the  $z$  axis coincides with the  $c$  axis, the summations of the first two terms and the third term are taken over NN pairs on the same intercalate layer and on the adjacent intercalate layers, respectively. In this expression,  $J$  is the ferromagnetic intraplanar exchange interaction,  $J_A$  is the anisotropic exchange interaction showing XY anisotropy, and  $J'$  is the antiferromagnetic interplanar exchange interaction. The NNN antiferromagnetic intraplanar exchange interaction is not included in Eq. (1). These parameters for stage-2  $\text{CoCl}_2$  GIC and  $\text{CoCl}_2$  are summarized in Table I. The value of  $J$  is estimated from the value of Curie-Weiss temperature  $\Theta$  by the relation  $J = 3\Theta / [2zS(S+1)] = \Theta/3$ , where the fictitious spin

TABLE I. Magnetic properties of stage-2  $\text{CoCl}_2$  GIC and pristine  $\text{CoCl}_2$ . The values of  $J$  are estimated from  $\Theta$ :  $J = \Theta/3$ .  $g_a$  is the  $g$  factor along the direction perpendicular to the  $c$  axis.

Stage-2 $\text{CoCl}_2$ GIC		$\text{CoCl}_2$	
$S$	1/2	$S$	1/2
$g_a$	6.36	$g_a$	6.65
$J$ (K)	9.04	$J$ (K)	13.54
$J_A$ (K)	3.72	$J_A$ (K)	8.0
$J'$ (K)	$-8 \times 10^{-4}$	$J'$ (K)	$-1.08$
$T_{\text{cl}}$ (K)	8.2	$T_N$ (K)	24.5
$T_{\text{cu}}$ (K)	9.1		
$\Theta$ (K)	27.12	$\Theta$ (K)	40.63
$P_{\text{eff}}$ ( $\mu_B$ )	5.51	$P_{\text{eff}}$ ( $\mu_B$ )	5.76

$S = 1/2$  and the number of NN atoms  $z = 6$ . Upon intercalation, the ferromagnetic intraplanar exchange interaction does not change drastically, but the antiferromagnetic interplanar exchange interaction is greatly reduced.

The pristine  $\text{CoCl}_2$  orders antiferromagnetically at  $T_N = 24.5 \text{ K}$ , with the  $\text{Co}^{2+}$  spins lying within the 2D ferromagnetic layers which are antiferromagnetically stacked along the  $c$  axis.<sup>14</sup> The stage-2  $\text{CoCl}_2$  GIC undergoes two magnetic phase transitions at  $T_{\text{cl}} = 8.2 \text{ K}$  and  $T_{\text{cu}} = 9.1 \text{ K}$ .<sup>1</sup> The intermediate phase between  $T_{\text{cl}}$  and  $T_{\text{cu}}$  has a purely 2D long-range spin ordering. There is no spin correlation between the adjacent intercalate layers. Below  $T_{\text{cl}}$ , there occurs 3D antiferromagnetic ordering where the 2D ferromagnetic layers are antiferromagnetically stacked along the  $c$  axis. The high-temperature phase above  $T_{\text{cu}}$  is paramagnetic. The finite size of the islands may be a crucial element in the two-step spin ordering in stage-2  $\text{CoCl}_2$  GIC. The pristine  $\text{CoCl}_2$  has a homogeneous  $\text{CoCl}_2$  layer with infinite island size. In this case, a weak interplanar exchange interaction  $J'$ , no matter how small, causes the 2D and 3D spin orderings to occur at the same temperature  $T_N (= 24.5 \text{ K})$ . In stage-2  $\text{CoCl}_2$  GIC, the growth of the in-plane spin correlation may be limited by the existence of islands, making the effective interplanar exchange interaction finite and suppressing the 3D spin ordering to a lower temperature than the 2D spin ordering temperature.

## III. EXPERIMENTAL PROCEDURE

The dehydration of  $\text{CoCl}_2$  and  $\text{MgCl}_2$  was done at  $400^\circ\text{C}$  in the presence of HCl gas at one atmosphere. Single crystals of  $\text{Co}_c\text{Mg}_{1-c}\text{Cl}_2$  over the entire range of Co concentrations are grown by using the Bridgman method: a mixture of dehydrated  $\text{CoCl}_2$  and  $\text{MgCl}_2$ , with nominal weight composition, was heated in quartz sealed in vacuum at  $990^\circ\text{C}$ . Stage-2  $\text{Co}_c\text{Mg}_{1-c}\text{Cl}_2$  GICs were synthesized by intercalation of single-crystal  $\text{Co}_c\text{Mg}_{1-c}\text{Cl}_2$  into single-crystal kish graphite in a chlorine gas atmosphere at a pressure of 740 Torr. The reaction was continued at  $540^\circ\text{C}$  for 20 days.

The (00L) x-ray diffraction of stage-2  $\text{Co}_c\text{Mg}_{1-c}\text{Cl}_2$  GIC was measured at 300 K by using a Huber double-

circle diffractometer with a Mo  $K\alpha$  x-ray radiation source (1.5 kW) and HOPG monochromator. An entrance slit of  $2 \times 2 \text{ mm}^2$  was placed between the monochromator and the sample. The x-ray beam diffracted by the sample was collimated by an exit slit of  $1 \times 1 \text{ mm}^2$  and detected by a Bicorn photomultiplier tube. The dc magnetic susceptibility of  $\text{Co}_c\text{Mg}_{1-c}\text{Cl}_2$  and stage-2  $\text{Co}_c\text{Mg}_{1-c}\text{Cl}_2$  GIC was measured by the Faraday balance method in the temperature range between 1.5 and 300 K. A magnetic field of  $100 \text{ Oe} \leq H \leq 2 \text{ kOe}$  was applied in an arbitrary direction in the  $c$  plane of the samples. The ac magnetic susceptibility of stage-2  $\text{Co}_c\text{Mg}_{1-c}\text{Cl}_2$  GIC was measured by a conventional ac Hartshorn bridge method in the temperature range between 2.6 and 12 K. An ac magnetic field of 330 Hz was applied in an arbitrary direction in the  $c$  plane of the samples.

#### IV. RESULT

##### A. Pristine $\text{Co}_c\text{Mg}_{1-c}\text{Cl}_2$

We have measured the dc magnetic susceptibility of  $\text{Co}_c\text{Mg}_{1-c}\text{Cl}_2$  with  $c = 0.35, 0.4, 0.45, 0.5, 0.55, 0.6, 0.65, 0.7, 0.75, 0.8, 0.85, 0.9, 0.95,$  and 1 at  $H = 2 \text{ kOe}$  in the temperature range between 25 and 300 K. Here  $c$  is the nominal Co concentration: the  $\text{Co}_c\text{Mg}_{1-c}\text{Cl}_2$  sample was prepared from a mixture with a nominal weight composition of  $c \text{ CoCl}_2$  and  $(1-c) \text{ MgCl}_2$ . The dc magnetic susceptibility is found to obey the Curie-Weiss law

$$\chi = \frac{C_M}{T - \Theta} + \chi_0, \quad (2)$$

above 150 K, where  $C_M$  is the Curie-Weiss constant,  $\Theta$  is the Curie-Weiss temperature, and  $\chi_0$  is a temperature-independent susceptibility. The least-squares fit of our susceptibility data for  $150 \text{ K} \leq T \leq 300 \text{ K}$  to Eq. (2) yields the  $\Theta$ ,  $C_M$ , and  $\chi_0$ . Figure 1 shows the plots of reciprocal susceptibility  $(\chi - \chi_0)^{-1}$  as a function of temperature for  $\text{Co}_c\text{Mg}_{1-c}\text{Cl}_2$  with  $c = 0.5, 0.8,$  and 1. The deviation from the Curie-Weiss law is indicative of the appearance of short-range order below 150 K. The values of Curie-Weiss temperature  $\Theta$  and the effective magnetic moment  $P_{\text{eff}}$  for  $\text{Co}_c\text{Mg}_{1-c}\text{Cl}_2$  samples are listed in Table II. Here the values of  $P_{\text{eff}} (\mu_B/\text{av atom})$  are estimated from the relation  $C_M = N_A^2 \mu_B^2 P_{\text{eff}}^2 / 3k_B \approx P_{\text{eff}}^2 / 8$ , where  $N_A$  is Avogadro's number,  $\mu_B$  is the Bohr magneton, and  $k_B$  is the Boltzmann constant.

For the ideal system of  $\text{Co}_c\text{Mg}_{1-c}\text{Cl}_2$  with Co concentration  $c$ , the concentration dependence of  $\Theta(c)$  and  $P_{\text{eff}}(c)$  are predicted from the molecular field theory as

$$\Theta(c) = c\Theta(c=1) \quad (3)$$

and

$$P_{\text{eff}}(c) = \sqrt{c} P_{\text{eff}}(c=1), \quad (4)$$

respectively, where the  $\text{Co}^{2+}$  and  $\text{Mg}^{2+}$  ions are assumed to be randomly distributed on the triangular lattice sites. Figures 2 and 3 show the nominal Co concentration dependence of  $\Theta$  and  $P_{\text{eff}}$  for  $\text{Co}_c\text{Mg}_{1-c}\text{Cl}_2$ . In Fig. 2, our data for  $\Theta$  fit well with the solid line described by Eq.

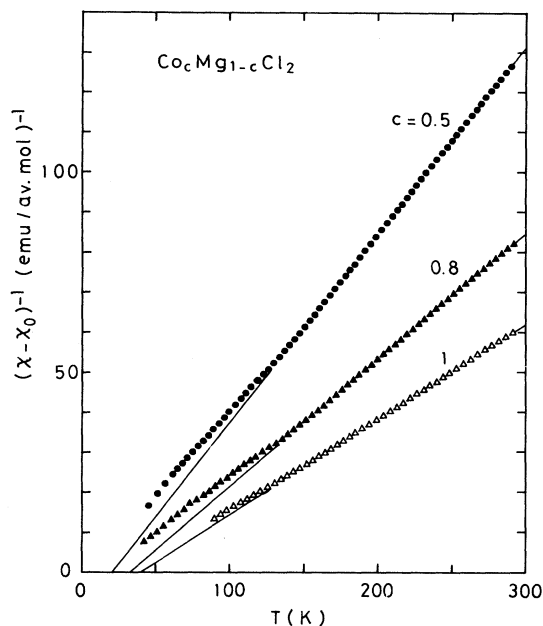


FIG. 1. Reciprocal susceptibility  $(\chi - \chi_0)^{-1}$  vs  $T$  for  $\text{Co}_c\text{Mg}_{1-c}\text{Cl}_2$  with  $c = 0.5$  ( $\bullet$ ),  $0.8$  ( $\blacktriangle$ ), and  $1$  ( $\triangle$ ), where  $\chi_0$  is a temperature-independent susceptibility. The solid line is a least-squares fit described by Eq. (2) with  $C_M$  and  $\Theta$  listed in Table II.

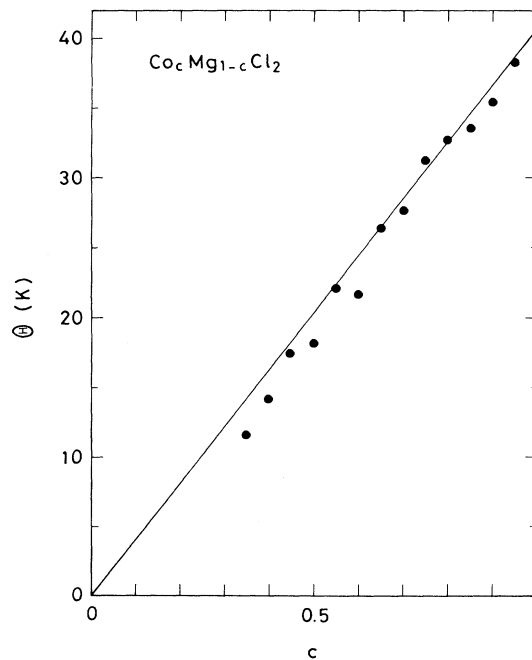


FIG. 2. Curie-Weiss temperature  $\Theta$  vs nominal Co concentration  $c$  for  $\text{Co}_c\text{Mg}_{1-c}\text{Cl}_2$ . The solid line is described by Eq. (3) with  $\Theta(c=1) = 40.63 \text{ K}$ .

TABLE II. Curie-Weiss temperature  $\Theta$ , effective magnetic moment  $P_{\text{eff}}$ , and Néel temperature  $T_N$  for  $\text{Co}_c\text{Mg}_{1-c}\text{Cl}_2$ .

Sample name	$c$	$\Theta$ (K)	$P_{\text{eff}}$ ( $\mu_B/\text{av atom}$ )	$T_N$ (K)	$\chi_{\text{max}}$ (emu/Co mol)
1	1.0	40.630±0.125	5.76	24.5	0.45
2	0.95	38.315±0.122	5.60		
3	0.9	35.460±0.048	5.43	20.2	0.49
4	0.85	33.596±0.342	5.26		
5	0.8	32.756±0.226	5.12	16.6	0.56
6	0.75	31.341±0.310	4.99		
7	0.7	27.578±0.070	4.82	12.7	0.72
8	0.65	26.424±0.046	4.63		
9	0.6	21.631±0.197	4.20	9.3	
10	0.55	22.169±0.077	4.18	6.8	0.91
11	0.5	18.126±0.092	3.90	5.7	1.10
12	0.45	17.559±0.068	3.82		
13	0.4	14.210±0.144	3.59		
14	0.35	11.665±0.090	3.35		

(3) with  $\Theta(c=1)=40.63$  K, which is larger than that reported by Starr *et al.*<sup>15</sup> ( $=38.1$  K). A positive sign for  $\Theta$  indicates that the average intraplanar exchange interaction is ferromagnetic at least for  $c \geq 0.35$ . In Fig. 3, our data for  $P_{\text{eff}}$  are in good agreement with the solid line described by Eq. (4) with  $P_{\text{eff}}(c=1)=5.76$  ( $\mu_B/\text{Co atom}$ ). Then it is concluded from these results that (i) the actual Co concentration of  $\text{Co}_c\text{Mg}_{1-c}\text{Cl}_2$  is the same as the nominal Co concentration, and that (ii)  $\text{Co}^{2+}$  and  $\text{Mg}^{2+}$  ions are randomly distributed on the triangular lattice sites.

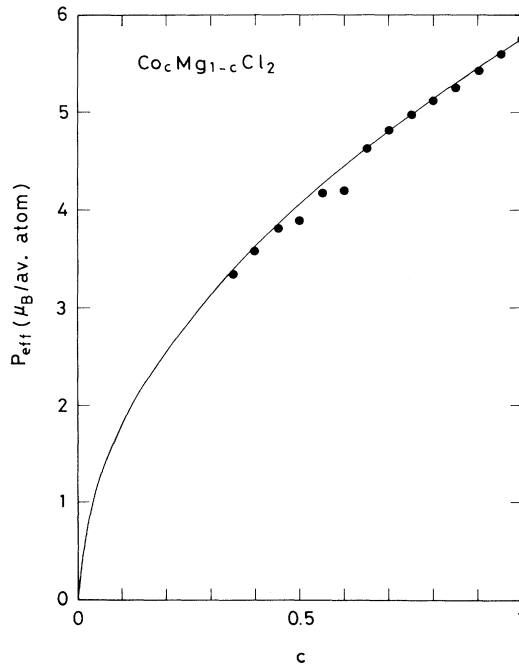


FIG. 3. Effective magnetic moment  $P_{\text{eff}}$  ( $\mu_B/\text{av atom}$ ) vs nominal Co concentration  $c$  for  $\text{Co}_c\text{Mg}_{1-c}\text{Cl}_2$ . The solid line is described by Eq. (4) with  $P_{\text{eff}}(c=1)=5.76\mu_B/\text{Co atom}$ .

We have also measured the dc magnetic susceptibility of  $\text{Co}_c\text{Mg}_{1-c}\text{Cl}_2$  with  $c=0.5, 0.55, 0.6, 0.7, 0.8, 0.9,$  and  $1$  at  $H=500$  Oe in the temperature range  $4.7 \text{ K} \leq T \leq 30$  K. Figure 4 shows the temperature dependence of dc magnetic susceptibility  $\chi$  (emu/Co mol) of  $\text{Co}_c\text{Mg}_{1-c}\text{Cl}_2$  with  $c=0.5, 0.7, 0.8,$  and  $1$ . Each susceptibility shows a broad peak at the Néel temperature listed in Table II. The peak susceptibility monotonically increases with decreasing Co concentration and reaches  $1.1$  emu/Co mol for  $c=0.5$ . This concentration dependence of the peak susceptibility will be discussed in terms of scaling theory

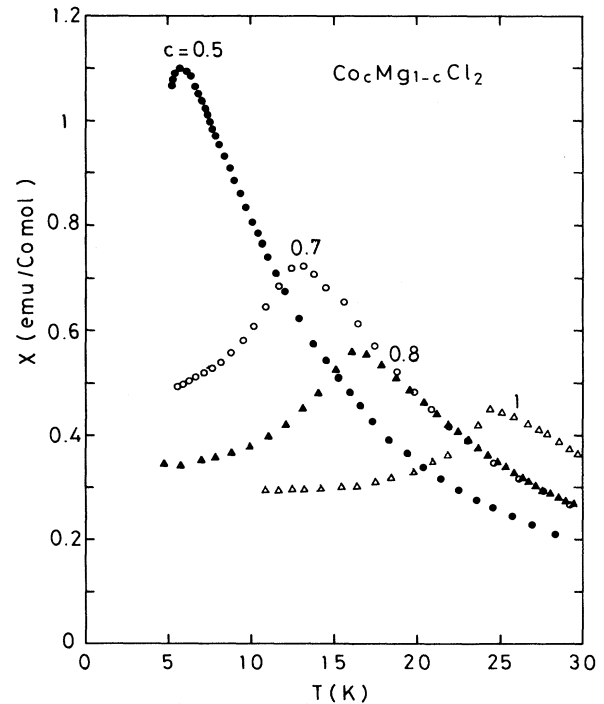


FIG. 4. Temperature dependence of  $\chi$  for  $\text{Co}_c\text{Mg}_{1-c}\text{Cl}_2$  with  $c=0.5, 0.7, 0.8,$  and  $1$ .  $H=500$  Oe and  $H \perp c$ .

in Sec. V.

Figure 5 shows the Co concentration dependence of Néel temperature for  $\text{Co}_c\text{Mg}_{1-c}\text{Cl}_2$ . In the present work we obtain  $T_N(c=1)=24.5$  K, which is slightly different from that reported by Wilkinson *et al.* (24.9 K).<sup>14</sup> The Néel temperature decreases linearly with decreasing Co concentration. The reduced limiting slope  $\sigma$  of  $\text{Co}_c\text{Mg}_{1-c}\text{Cl}_2$  is obtained from Fig. 5 as

$$\sigma = \left[ \frac{1}{T_N(c)} \frac{dT_N(c)}{dc} \right]_{c=1} = 1.563. \quad (5)$$

This value of  $\sigma$  is compared with that of site-diluted Ising antiferromagnet  $\text{Fe}_c\text{Mg}_{1-c}\text{Cl}_2$  ( $\sigma=1.45$ ).<sup>16</sup> The magnetic ordered structure of  $\text{Fe}_c\text{Mg}_{1-c}\text{Cl}_2$  is composed of 2D ferromagnetic layers with spins aligned along the  $c$  axis, the layers being antiferromagnetically stacked along the  $c$  axis. As far as we know, there has been no report on the theoretical value of  $\sigma$  for the site-diluted XY model on the triangular lattice. For the site-diluted Ising model on the triangular lattice, the value of  $\sigma$  is predicted as  $1.47 \pm 0.02$  by Ching and Huber,<sup>17</sup> which explains well the value of  $\sigma$  for  $\text{Fe}_c\text{Mg}_{1-c}\text{Cl}_2$ . Our result for  $\sigma$  is a little larger than the theoretical value of  $\sigma$  for the Ising model, indicating that the value of  $\sigma$  may increase with the degree of spin symmetry for systems with the same lattice.

The percolation threshold  $c_p$  defined as the concentration where this straight line for  $T_N$  vs  $c$  intersects the axis of concentration is estimated as  $c_p=0.36$  for  $\text{Co}_c\text{Mg}_{1-c}\text{Cl}_2$ , which is close to the value reported by

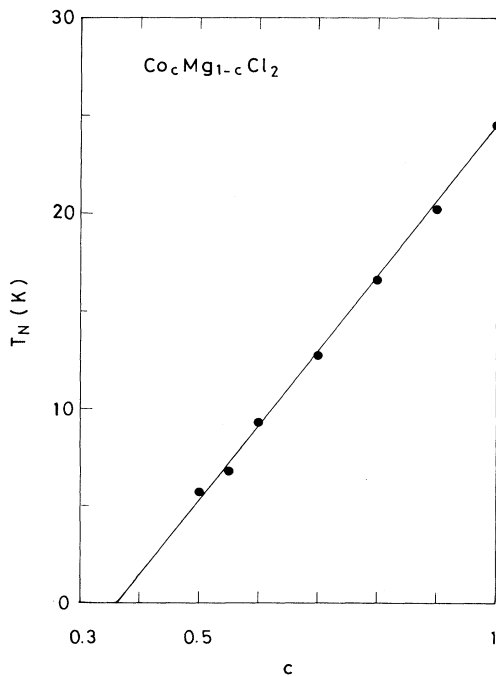


FIG. 5. Néel temperature  $T_N$  vs  $c$  for  $\text{Co}_c\text{Mg}_{1-c}\text{Cl}_2$ . The straight line is a least-squares fit described by Eq. (5).

Katsumata *et al.*<sup>7</sup> ( $c_p=0.3$ ). They have shown from the electron-spin resonance measurement at 4.2 K that the saturation magnetic field at which the transition occurs between the antiferromagnetic phase and the ferromagnetic phase decreases with decreasing Co concentration and tends to zero around  $c_p=0.3$ . The value of  $c_p$  depends on the lattice, on the range of exchange interactions, and on the type of dilution (site or bond). The value of  $c_p$  is theoretically predicted as 0.5, 0.295, and 0.225 for the site-diluted triangular lattice with only NN interaction, with NN and NNN interactions, and with NN, NNN, and third NN interactions, respectively.<sup>18</sup> Our result of  $c_p=0.36$  suggests the possibility that there is a competition between the NN ferromagnetic and the NNN antiferromagnetic intraplanar exchange interactions in  $\text{Co}_c\text{Mg}_{1-c}\text{Cl}_2$ , which may give rise to an XY spin-glass behavior. In fact,  $\text{Fe}_c\text{Mg}_{1-c}\text{Cl}_2$  is found to show an Ising spin-glass behavior in the concentration range  $0.3 \leq c \leq 0.6$  because of such a competition. The concentration dependence of Néel temperature in  $\text{Fe}_c\text{Mg}_{1-c}\text{Cl}_2$  is very similar to that in  $\text{Co}_c\text{Mg}_{1-c}\text{Cl}_2$ :  $T_N(c)$  decreases with decreasing Fe concentration for  $0.55 \leq c \leq 1.0$ . The percolation threshold where the straight line intersects the concentration axis is obtained as  $c_p \approx 0.33$ , which is very close to our result for  $c_p$  of  $\text{Co}_c\text{Mg}_{1-c}\text{Cl}_2$ .

## B. Stage-2 $\text{Co}_c\text{Mg}_{1-c}\text{Cl}_2$ GIC

Nicholls and Dresselhaus<sup>6</sup> have determined the Co concentration of stage-1  $\text{Co}_c\text{Mg}_{1-c}\text{Cl}_2$  GIC by electron microprobe measurements. The chemical analysis of the electron microprobe extends over a limited region which is about  $2 \mu\text{m}$  in diameter and  $2 \mu\text{m}$  in depth below the sample surface. The Co concentration thus determined may be the average value near the sample surface, not the average value over the whole GIC sample. In the present work, we use a different method to determine the Co concentration  $c$  over the macroscopic scale of stage-2  $\text{Co}_c\text{Mg}_{1-c}\text{Cl}_2$  GIC samples. The Co concentration  $c$  is determined by the ratio of  $\Theta$  of stage-2  $\text{Co}_c\text{Mg}_{1-c}\text{Cl}_2$  GIC to that of stage-2  $\text{CoCl}_2$  GIC:  $c = \Theta / \Theta(c=1)$ . Here we assume that the Co concentration  $c$  of stage-2  $\text{Co}_c\text{Mg}_{1-c}\text{Cl}_2$  GIC may be different from the Co concentration  $c_b$  of the pristine compound used as an intercalant. In this case, the Co concentration  $c$  may be related to  $c_b$  by<sup>19</sup>

$$\frac{c}{1-c} \left[ \frac{1-c_b}{c_b} \right] = \lambda, \quad (6)$$

where  $\lambda$  is an equilibrium constant:  $c > c_b$  for  $\lambda > 1$  and  $c < c_b$  for  $\lambda < 1$ . For convenience, the sample of stage-2  $\text{Co}_c\text{Mg}_{1-c}\text{Cl}_2$  GIC is denoted by the Co concentration  $c_b$  of pristine compound used as an intercalant, until the Co concentration  $c$  of stage-2  $\text{Co}_c\text{Mg}_{1-c}\text{Cl}_2$  GIC is determined.

We have measured the dc magnetic susceptibility of stage-2  $\text{Co}_c\text{Mg}_{1-c}\text{Cl}_2$  GIC with the nominal Co concentration  $c_b=0.4, 0.55, 0.6, 0.65, 0.75, 0.8, 0.9, 0.95$ , and 1 at  $H=2$  kOe in the temperature range  $20 \text{ K} \leq T \leq 300 \text{ K}$ .

TABLE III. Curie-Weiss temperature  $\Theta$ , effective magnetic moment  $P_{\text{eff}}$ , and d spacing ( $\text{\AA}$ ) for stage-2  $\text{Co}_c\text{Mg}_{1-c}\text{Cl}_2$  GIC with stoichiometry  $\text{C}_n\text{Co}_c\text{Mg}_{1-c}\text{Cl}_2$ . Here  $c_b$  is the nominal Co concentration which is equal to the concentration of intercalant.  $T_c = T_{\text{cl}}$  at  $c = 1$ .

Sample name	$c_b$	$c$	$n$	$\Theta$ (K)	$P_{\text{eff}}$ ( $\mu_B/\text{av atom}$ )	d spacing ( $\text{\AA}$ )	$T_c$ (K)
1		1.0	8.90	$27.12 \pm 0.12$	5.51	$12.789 \pm 0.013$	8.20
2	0.95	0.99	10.2	$26.73 \pm 0.12$	5.66		8.64
3	0.9	0.95	11.7	$25.71 \pm 0.35$	5.69		7.78
4	0.8	0.88	14.7	$23.77 \pm 0.24$	5.20	$12.765 \pm 0.413$	7.76
5	0.75	0.84	14.2	$22.73 \pm 0.16$	5.71	$12.765 \pm 0.426$	6.74
6	0.65	0.74	13.3	$20.11 \pm 0.06$	5.28	$12.840 \pm 0.236$	5.06
7	0.6	0.65	11.7	$17.75 \pm 0.25$	4.89		3.56
8	0.55	0.61	11.7	$16.48 \pm 0.32$	4.23	$12.802 \pm 0.277$	2.82
9	0.4	0.46	11.8	$12.53 \pm 0.43$	4.35	$12.860 \pm 0.093$	

The susceptibility is found to obey the Curie-Weiss law above 150 K. The least-squares fit of our susceptibility data for  $150 \text{ K} \leq T \leq 300 \text{ K}$  to Eq. (2) yields the value of  $\Theta$  listed in Table III. Figure 6 shows the reciprocal susceptibility  $(\chi - \chi_0)^{-1}$  as a function of temperature for the compound with  $c_b = 0.8$ . The solid straight line is a least-squares fit described by Eq. (2) with  $\Theta = 23.77 \text{ K}$ . Figure 7 shows the nominal Co concentration dependence of  $\Theta$  for stage-2  $\text{Co}_c\text{Mg}_{1-c}\text{Cl}_2$  GIC. The Curie-Weiss temperature  $\Theta$  slightly deviates upward from the straight line described by Eq. (3) with  $\Theta(c=1) = 27.12 \text{ K}$ , which is different from that reported by Wiesler *et al.* (23.2 K).<sup>12</sup> This result shows that the actual Co concen-

tration  $c$  of stage-2  $\text{Co}_c\text{Mg}_{1-c}\text{Cl}_2$  GIC is a little larger than the nominal Co concentration  $c_b$ . The actual Co concentration of stage-2  $\text{Co}_c\text{Mg}_{1-c}\text{Cl}_2$  GIC determined from the relation  $c = \Theta/\Theta(c=1)$  is listed in Table III. Our result,  $c > c_b$ , is consistent with the fact that  $\text{MgCl}_2$  is a more difficult compound to intercalate into graphite under the same condition than  $\text{CoCl}_2$ . Note that the value of  $\lambda$  decreases monotonically from 5.21 to 1.28 as  $c$  decreases from 0.99 to 0.46. Hereafter, we denote the sample of stage-2  $\text{Co}_c\text{Mg}_{1-c}\text{Cl}_2$  GIC by the actual Co concentration  $c$ . The effective magnetic moment  $P_{\text{eff}}$  ( $\text{emu}/\text{av atom}$ ) for each sample can be estimated by using the value of  $c$  and is listed in Table III.

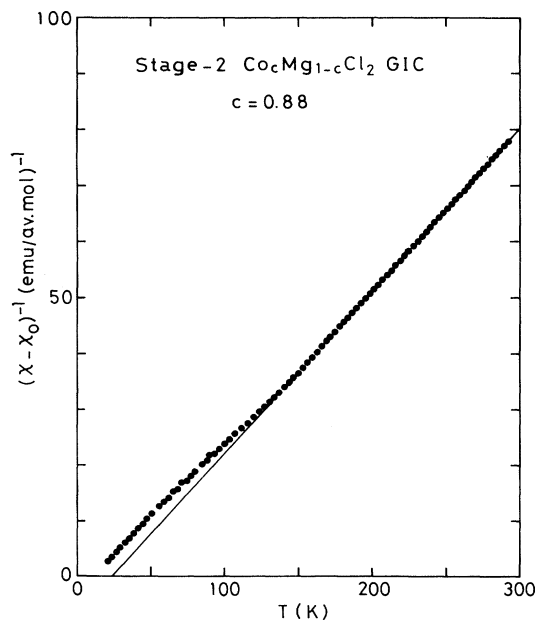


FIG. 6. Reciprocal susceptibility  $(\chi - \chi_0)^{-1}$  vs  $T$  for stage-2  $\text{Co}_c\text{Mg}_{1-c}\text{Cl}_2$  GIC with nominal Co concentration  $c_b = 0.88$  (sample No. 4 with  $c = 0.88$ ).  $H = 500 \text{ Oe}$  and  $\mathbf{H} \perp \mathbf{c}$ . The solid line is a least-squares fit described by Eq. (2) with  $c_M$  and  $\Theta$  listed in Table III.

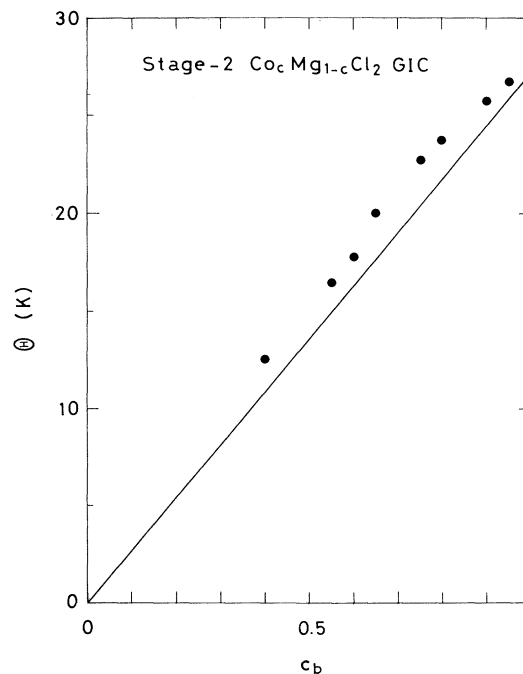


FIG. 7. Curie-Weiss temperature  $\Theta$  vs nominal Co concentration  $c_b$  for stage-2  $\text{Co}_c\text{Mg}_{1-c}\text{Cl}_2$  GIC. The solid line is described by Eq. (3) with  $\Theta(c=1) = 27.12 \text{ K}$ .

We have measured the  $(00L)$  x-ray diffraction of stage-2  $\text{Co}_c\text{Mg}_{1-c}\text{Cl}_2$  GIC at 300 K. Figure 8 shows a typical example of the  $(00L)$  x-ray diffraction pattern for stage-2  $\text{Co}_c\text{Mg}_{1-c}\text{Cl}_2$  GIC with  $c=0.74$  (sample No. 6 in Table III), where  $Q_c$  is a scattering wave vector along the  $c^*$  axis. The Bragg reflections appear at  $Q_c = (2\pi/d)L$  ( $L=1, 2, \dots$ ) where  $d$  is the  $c$  axis repeat distance or simply  $d$  spacing ( $d=12.840 \text{ \AA}$ ). The values of  $d$  spacing for stage-2  $\text{Co}_c\text{Mg}_{1-c}\text{Cl}_2$  GIC are listed in Table III. Figure 9 shows the  $d$  spacing vs Co concentration for stage-2  $\text{Co}_c\text{Mg}_{1-c}\text{Cl}_2$  GIC. A large uncertainty of  $d$  spacing is due to the Hendricks-Teller type stage disorder characterized by the oscillation of the peak shift and full width at half-maximum of Bragg reflections with the Bragg index of majority stage.<sup>20</sup> All samples used in the present work were composed of a random arrangement of the majority packages of stage-2 and minority packages of stage-3 along the  $c$  axis. For sample No. 6 (Table III) with  $c=0.74$ , there are 80% of stage-2 packages and 20% of stage-3 packages. In spite of this uncertainty, the relationship between  $d$  spacing and  $c$  seems to follow the Vegard's law: the  $d$  spacing changes linearly with the Co concentration. This result suggests that Co and Mg ions are randomly distributed on the triangular lattice sites within the intercalate layer. As far as we know, there has been no report on the  $d$  spacing of stage-2  $\text{MgCl}_2$  GIC. However, the value of  $d$  at  $c=0$  is estimated as  $12.92 \text{ \AA}$  from the extrapolation of  $d$  vs  $c$  in Fig. 9. This value of  $d$  is larger than a sum of the  $d$  spacings of stage-1  $\text{MgCl}_2$  GIC ( $9.50 \text{ \AA}$ )<sup>6</sup> and pristine graphite ( $3.35 \text{ \AA}$ ).

We have measured the dc magnetic susceptibility of stage-2  $\text{Co}_c\text{Mg}_{1-c}\text{Cl}_2$  GIC with various Co concentrations at  $H=100 \text{ Oe}$  in the temperature range  $1.5 \text{ K} \leq T \leq 15 \text{ K}$ . The measured dc susceptibility coincides with the ratio of the magnetization  $M$  to the magnetic field  $H$ . Figure 10 shows the temperature variation of  $M/H$  (emu/Co mol) for stage-2  $\text{Co}_c\text{Mg}_{1-c}\text{Cl}_2$  GIC with  $c=0.47, 0.86$ , and 1. For  $c=0.86$ , for example, the mag-

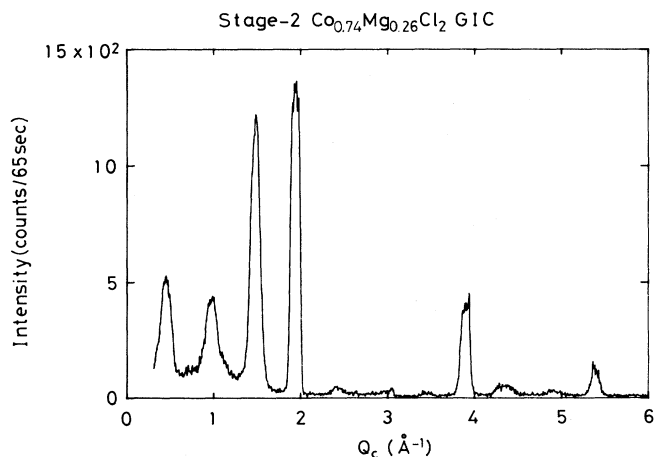


FIG. 8.  $(00L)$  x-ray diffraction pattern of stage-2  $\text{Co}_c\text{Mg}_{1-c}\text{Cl}_2$  GIC with  $c=0.74$  (Sample No. 6) at 300 K.  $Q_c = L(2\pi/d)$  with  $d=12.840 \text{ \AA}$ .

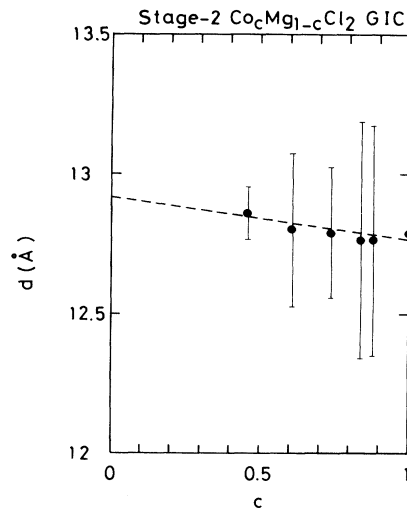


FIG. 9.  $d$  spacing vs Co concentration  $c$  for stage-2  $\text{Co}_c\text{Mg}_{1-c}\text{Cl}_2$  GIC at 300 K.

netization  $M$  rapidly increases with decreasing temperature below 10 K, and reaches a saturated value of 90 emu/Co mol around 4 K, which is much larger than the peak value of  $\chi$  for  $\text{Co}_c\text{Mg}_{1-c}\text{Cl}_2$  ( $\approx 1.1 \text{ emu/Co mol}$ ).

The temperature dependence of magnetization  $M$  near the critical temperature is described by the smeared power law. The critical temperature is assumed to have a Gaussian distribution with average critical temperature  $\langle T_c \rangle$  and width  $\Delta T_c$ . The values of  $\langle T_c \rangle$  and  $\Delta T_c$  are

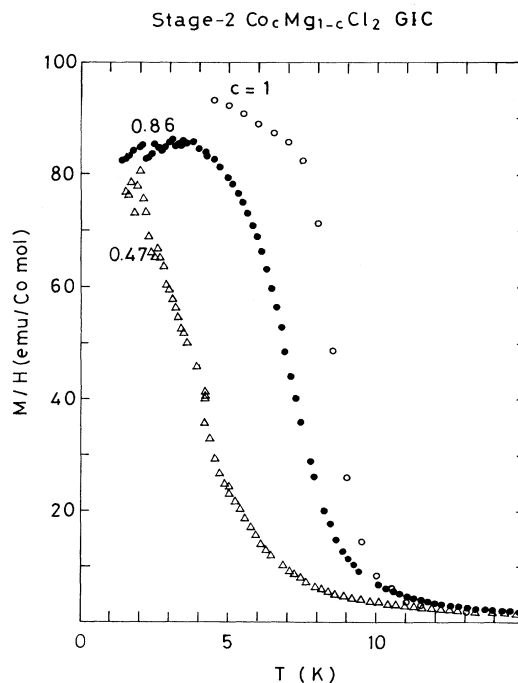


FIG. 10. Temperature dependence of  $\chi (=M/H)$  for stage-2  $\text{Co}_c\text{Mg}_{1-c}\text{Cl}_2$  GIC with  $c=0.47, 0.86$ , and 1, where  $H=100 \text{ Oe}$  and  $H \perp c$ .

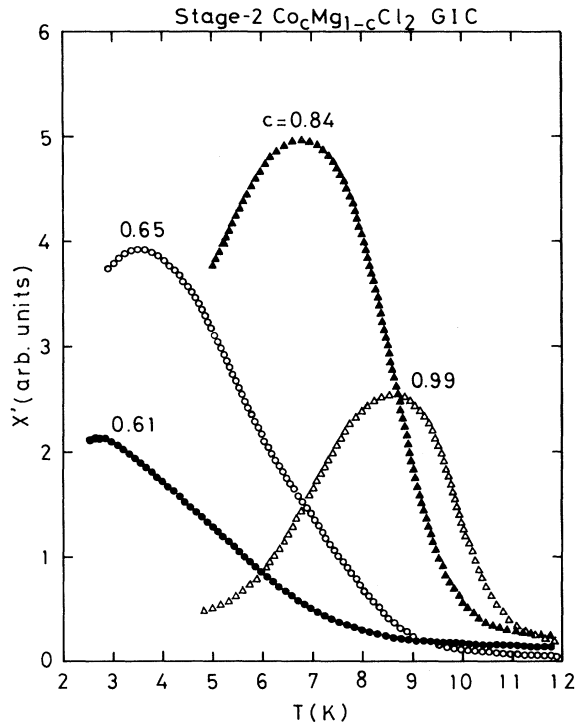


FIG. 11. Real part of ac magnetic susceptibility ( $\chi'$ ) vs  $T$  for stage-2  $\text{Co}_c\text{Mg}_{1-c}\text{Cl}_2$  GIC with  $c=0.61, 0.65, 0.84,$  and  $0.99$ . An ac magnetic field of  $\nu=330$  Hz and  $h=300$  mOe is applied along the  $c$  plane.

determined from the least-squares fits as  $\langle T_c \rangle = 6.95$  K and  $\Delta T_c = 1.18$  K for  $c=0.86$ , and  $\langle T_c \rangle = 8.78$  K and  $\Delta T_c = 0.62$  for  $c=1$ . The value of  $\Delta T_c$  is found to increase with decreasing Co concentration. For  $c=0.47$ , the magnetization monotonically increases with decreasing temperature like a paramagnetic susceptibility, indicating no magnetic phase transition at least above 2 K.

In order to determine the magnetic phase diagram of  $T_c$  vs  $c$ , we have measured the ac magnetic susceptibility of stage-2  $\text{Co}_c\text{Mg}_{1-c}\text{Cl}_2$  GIC with  $c=0.46, 0.61, 0.65, 0.74, 0.84, 0.88, 0.95, 0.99,$  and  $1$  in the temperature range  $2.6 \text{ K} \leq T \leq 12 \text{ K}$ . Figure 11 shows the temperature dependence of the real part of ac magnetic susceptibility for stage-2  $\text{Co}_c\text{Mg}_{1-c}\text{Cl}_2$  GIC with  $c=0.61, 0.65, 0.84,$  and  $0.99$ . The ac susceptibility for  $c=1$  shows a broad peak at 8.2 K corresponding to the lower critical temperature  $T_{c1}$ .<sup>1</sup> The critical temperature  $T_c$  shifts to the lower temperature side with decreasing Co concentration. Even for  $c=0.61$ , the ac susceptibility still shows a small peak at 2.82 K. For  $c=0.46$ , no peak is observed above 2.6 K for  $c=0.46$ . It is concluded from these results that the percolation threshold is between 0.46 and 0.61. This is consistent with the prediction of  $c_p=0.5$  for the 2D triangular lattice with NN interactions.

## V. DISCUSSION

The difference between magnetic properties of  $\text{Co}_c\text{Mg}_{1-c}\text{Cl}_2$  and stage-2  $\text{Co}_c\text{Mg}_{1-c}\text{Cl}_2$  GIC arises

mainly from that between their characteristic layered structures. The ratio of  $|J'|$  to  $J$  in  $\text{Co}_c\text{Mg}_{1-c}\text{Cl}_2$  ( $|J'/J| \approx 0.1$ ) is much larger than that in stage-2  $\text{Co}_c\text{Mg}_{1-c}\text{Cl}_2$  GIC ( $|J'/J| \approx 10^{-3}$ ). The  $\text{Co}_c\text{Mg}_{1-c}\text{Cl}_2$  layers of the pristine  $\text{Co}_c\text{Mg}_{1-c}\text{Cl}_2$  are structurally homogeneous, while the  $\text{Co}_c\text{Mg}_{1-c}\text{Cl}_2$  layers of stage-2  $\text{Co}_c\text{Mg}_{1-c}\text{Cl}_2$  GIC consist of small islands which are characteristic of acceptor-type GICs. In both systems, the effective antiferromagnetic coupling between adjacent  $\text{Co}_c\text{Mg}_{1-c}\text{Cl}_2$  layers is described by

$$J'_{\text{eff}} \approx S(S+1)(\xi/a_0)^2 J', \quad (7)$$

where  $\xi$  is the in-plane correlation length and  $a_0$  is the in-plane lattice constant. In  $\text{Co}_c\text{Mg}_{1-c}\text{Cl}_2$ , the value of  $|J'_{\text{eff}}|$  becomes of the same order of  $J$  near  $T_N$  because of relatively strong  $J'$  and the unlimited growth of  $\xi$ , giving rise to 3D spin ordering below  $T_N$ . In stage-2  $\text{Co}_c\text{Mg}_{1-c}\text{Cl}_2$  GIC, the value of  $|J'_{\text{eff}}|$  may be still smaller than  $J$  because of extremely weak  $J'$  and the limited growth of  $\xi$  by the size of islands near  $T_c$ , leading to 2D critical behavior just above  $T_c$ , although 3D spin ordering occurs below  $T_c$ . These results suggest that  $\text{Co}_c\text{Mg}_{1-c}\text{Cl}_2$  and stage-2  $\text{Co}_c\text{Mg}_{1-c}\text{Cl}_2$  GIC magnetically behave like site-diluted 3D XY and 2D XY spin systems, respectively.

Figure 12(a) shows the ratio  $R$  of the critical temperature to the Curie-Weiss temperature  $\Theta$  of  $\text{Co}_c\text{Mg}_{1-c}\text{Cl}_2$  and stage-2  $\text{Co}_c\text{Mg}_{1-c}\text{Cl}_2$  GIC as a function of Co concentration. The ratio  $T_N/\Theta$  of  $\text{Co}_c\text{Mg}_{1-c}\text{Cl}_2$  decreases from 0.60 to 0.31 as the concentration  $c$  decreases from  $c=1$  to  $c=0.5$ . The ratio  $T_c/\Theta$  of stage-2  $\text{Co}_c\text{Mg}_{1-c}\text{Cl}_2$  GIC decreases from 0.30 to 0.17 as the concentration  $c$  decreases from  $c=1$  to  $c=0.61$ . It is experimentally known that the value of  $R$  decreases as the dimensionality of the system decreases.<sup>21</sup> The value of  $R$  for  $\text{Co}_c\text{Mg}_{1-c}\text{Cl}_2$  is much larger than that for stage-2  $\text{Co}_c\text{Mg}_{1-c}\text{Cl}_2$  GIC for  $c \geq 0.7$ , indicating that  $\text{Co}_c\text{Mg}_{1-c}\text{Cl}_2$  and stage-2  $\text{Co}_c\text{Mg}_{1-c}\text{Cl}_2$  GIC approximate 3D and 2D spin systems, respectively. In the stage-2  $\text{Co}_c\text{Mg}_{1-c}\text{Cl}_2$  GIC, the value of  $R$  is assumed to be lower than 0.1 for  $0.5 \leq c < 0.55$ , indicating that the system approximates a 1D spin system. This result is consistent with a predicted 1D character near the percolation threshold; for a cluster shape with high ramification, the spin correlation from one end of the lattice to the other would propagate along a 1D chain. For example, the susceptibility of site-diluted quasi-2D XY ferromagnet  $\text{K}_2\text{Cu}_c\text{Zn}_{1-c}\text{F}_4$  with  $c=0.6$  ( $c_p=0.59$ ) is well described by the exact solution of the 1D Heisenberg ferromagnet with  $S=1/2$ .<sup>22</sup>

Figure 12(b) shows the plots of reduced critical temperature  $T_c(c)/T_c(1)$  vs Co concentration for  $\text{Co}_c\text{Mg}_{1-c}\text{Cl}_2$  and stage-2  $\text{Co}_c\text{Mg}_{1-c}\text{Cl}_2$  GIC, where  $T_c(1)=24.5$  K for  $\text{Co}_c\text{Mg}_{1-c}\text{Cl}_2$  and 8.2 K for stage-2  $\text{Co}_c\text{Mg}_{1-c}\text{Cl}_2$  GIC. The reduced critical temperature of  $\text{Co}_c\text{Mg}_{1-c}\text{Cl}_2$  falls on a straight line with an initial slope given by Eq. (5), at least for  $c \geq 0.5$ , and reduces to zero around  $c=0.36$ , which is close to the theoretical value ( $c_p=0.295$ ) for the 2D triangular lattice with NN and NNN exchange in-

teraction. The reduced critical temperature of stage-2  $\text{Co}_c\text{Mg}_{1-c}\text{Cl}_2$  GIC agrees well with the same straight line for  $c \geq 0.7$ , deviates from this straight line below  $c \approx 0.7$ , and seems to reduce to zero around  $c=0.5$ , which is theoretically predicted for the 2D triangular lattice with NN exchange interaction. The disappearance of NNN interaction in stage-2  $\text{Co}_c\text{Mg}_{1-c}\text{Cl}_2$  GIC is consistent with the fact that the value of  $J$  in stage-2  $\text{CoCl}_2$  is reduced 33% relative to that in  $\text{CoCl}_2$ . It is concluded from these results that (i) the effect of the dimensionality

on the dilution with Mg ions becomes important below  $c \approx 0.7$ , and that (ii) the effect of the NNN interaction on the dilution with Mg ions becomes significant below  $c \approx 0.5$ . The latter conclusion supports the result, derived by Katsumata *et al.*<sup>7</sup> for  $\text{Co}_c\text{Mg}_{1-c}\text{Cl}_2$ , that there may be a possibility of an XY spin-glass phase arising from the competition between ferromagnetic NN exchange interaction and antiferromagnetic NNN exchange interaction.

As described in Sec. IV, the susceptibility perpendicular to the  $c$  axis for  $\text{Co}_c\text{Mg}_{1-c}\text{Cl}_2$  shows a peak at the Néel temperature. This peak susceptibility  $\chi(T_N)$  increases with decreasing Co concentration. We find that the peak susceptibility of  $\text{Co}_c\text{Mg}_{1-c}\text{Cl}_2$  varies with its Néel temperature  $T_N(c)$  as

$$\chi(T_N) = A(T_N(c))^{-x}, \quad (8)$$

with  $x=1.1$  in the concentration range  $0.5 \leq c \leq 0.8$ , where  $A$  is constant. This result is similar to the results reported by Breed *et al.*<sup>23</sup> for quasi-2D antiferromagnet  $\text{K}_2\text{Mn}_c\text{Mg}_{1-c}\text{F}_4$  and 3D antiferromagnet  $\text{KMn}_c\text{Mg}_{1-c}\text{F}_3$ . The perpendicular susceptibility extrapolated to  $T=0$  is proportional to the inverse of the Néel temperature  $T_N(c)$ :  $x=1$ . Enoki and Tsujikawa<sup>24</sup> have also reported that the peak susceptibility of quasi-2D antiferromagnet  $\text{Ni}_c\text{Mg}_{1-c}(\text{OH})_2$  increases as the Néel temperature decreases. In this case the exponent  $x$  depends on the concentration range where the data are least-squares fitted to Eq. (8):  $x=0.94$ , for  $0.2 \leq c \leq 0.5$ , and  $x=2.02$  for  $0.1 \leq c \leq 0.3$  ( $c_p \approx 0.1$ ). The increase of peak susceptibility near the percolation threshold may be attributed to the paramagnetic susceptibility arising from isolated magnetic ions. The fraction of isolated magnetic ions increases with the dilution of nonmagnetic atoms. Another explanation for this effect, given by Harris and Kirkpatrick,<sup>25</sup> is that the balance of the two antiferromagnetic sublattices is destroyed by nonmagnetic atoms.

Now we discuss the value of  $x$  for  $\text{Co}_c\text{Mg}_{1-c}\text{Cl}_2$  in terms of recent scaling theory.<sup>26-28</sup> Near the percolation point ( $c=c_p, T=0$ ), which is the end of the critical line, the susceptibility  $\chi$  is assumed to be described by a scaling form

$$\chi(T, c-c_p) = |c-c_p|^{-\gamma_p} f\left(\frac{T}{|c-c_p|^\phi}\right), \quad (9)$$

where  $\phi$  is the percolation-crossover exponent, and  $\gamma_p$  is a percolation-critical exponent for susceptibility in approaching the percolation point along the  $T=0$  axis. The scaling function  $f(y)$  is assumed to have a peak value at  $y=y_0$ . In approaching the percolation point along the critical line defined by

$$T_N(c) = y_0 |c-c_p|^\phi, \quad (10)$$

the peak susceptibility  $\chi_{\max}$  is described by a scaling form

$$\chi_{\max} \approx |c-c_p|^{-\gamma_p} \approx (T_N(c))^{-\gamma_T}, \quad (11)$$

where  $\gamma_T (= \gamma_p/\phi)$  is the thermal-critical exponent of susceptibility in approaching a path along the  $c=c_p$  axis.

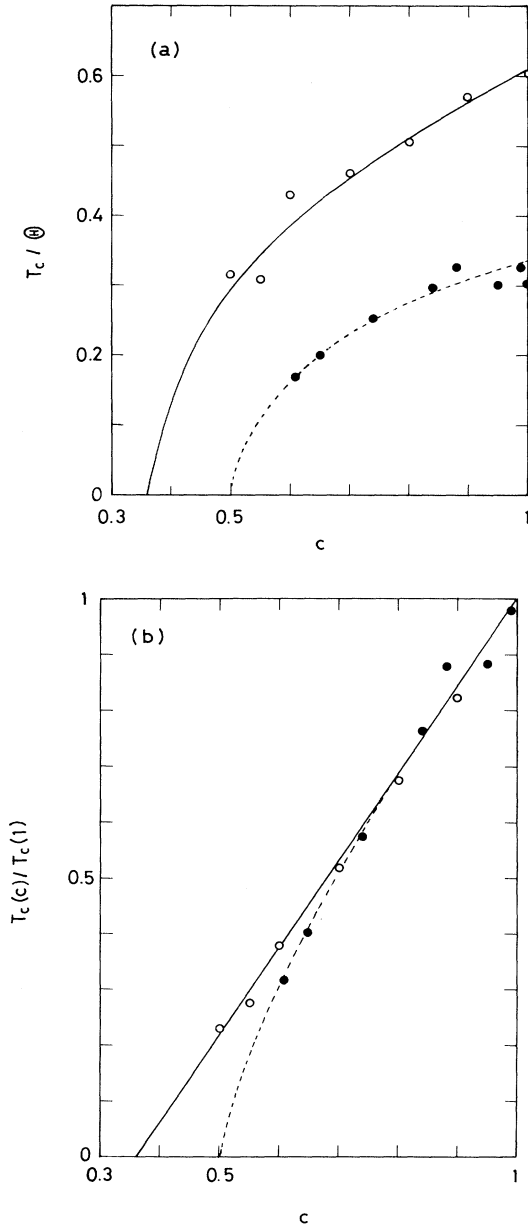


FIG. 12. (a)  $T_c(c)/\Theta(c)$  vs  $c$ , and (b) reduced critical temperature  $T_c(c)/T_c(1)$  vs  $c$  for stage-2  $\text{Co}_c\text{Mg}_{1-c}\text{Cl}_2$  GIC (●) and for  $\text{Co}_c\text{Mg}_{1-c}\text{Cl}_2$  (○). The solid and dotted lines are guides for the eye.

It is concluded from Eq. (11) that the value of  $x$  coincides with that of  $\gamma_T$ :  $\gamma_T = 1.1$  for  $\text{Co}_c\text{Mg}_{1-c}\text{Cl}_2$ . Experimental values of  $\gamma_T$  for several typical systems were obtained from neutron scattering measurements:  $\gamma_T = 2.4 \pm 0.1$  for  $\text{Rb}_2\text{Co}_c\text{Mg}_{1-c}\text{F}_4$  (2D Ising),<sup>29</sup>  $1.7 \pm 0.2$  for  $\text{Mn}_c\text{Zn}_{1-c}\text{F}_2$  (3D Ising),<sup>30</sup>  $1.50 \pm 0.15$  for  $\text{Rb}_2\text{Mn}_c\text{Mg}_{1-c}\text{F}_4$  (2D Heisenberg),<sup>31</sup> and  $1.73 \pm 0.15$  for  $\text{KMn}_c\text{Zn}_{1-c}\text{F}_3$  (3D Heisenberg).<sup>30</sup> As described above for  $\text{Ni}_c\text{Mg}_{1-c}(\text{OH})_2$ , the exponent  $x$  is likely to increase as the concentration range for the least-squares fits approaches the percolation threshold. For  $\text{Co}_c\text{Mg}_{1-c}\text{Cl}_2$  there are no data available of peak susceptibility vs  $T_N$  in the concentration range  $0.36 \leq c < 0.5$ . The value of  $\gamma_T$  derived from the data near the percolation threshold is expected to be larger than the result for  $\gamma_T$  ( $= 1.1$  for  $0.5 \leq c \leq 0.8$ ), which is consistent with the large value of  $\gamma_T$  derived from neutron scattering for typical compounds described above.

## VI. CONCLUSION

We have studied magnetic phase transitions of pristine  $\text{Co}_c\text{Mg}_{1-c}\text{Cl}_2$  and stage-2  $\text{Co}_c\text{Mg}_{1-c}\text{Cl}_2$  GIC. We have determined the Co concentration of  $\text{Co}_c\text{Mg}_{1-c}\text{Cl}_2$  and stage-2  $\text{Co}_c\text{Mg}_{1-c}\text{Cl}_2$  GIC from dc magnetic susceptibility. The Co concentration of  $\text{Co}_c\text{Mg}_{1-c}\text{Cl}_2$  is the same as the nominal Co concentration. On the other hand, the Co concentration of stage-2  $\text{Co}_c\text{Mg}_{1-c}\text{Cl}_2$  GIC is a little larger than the Co concentration of its intercalant, which is consistent with the fact that  $\text{MgCl}_2$  is a more difficult compound to intercalate into graphite under the same condition than  $\text{CoCl}_2$ . We have determined the magnetic phase diagram of  $\text{Co}_c\text{Mg}_{1-c}\text{Cl}_2$  and stage-2  $\text{Co}_c\text{Mg}_{1-c}\text{Cl}_2$  GIC from dc and ac magnetic susceptibility. The percolation threshold is  $c_p \approx 0.36$  for  $\text{Co}_c\text{Mg}_{1-c}\text{Cl}_2$ , which is close to the theoretical value ( $c_p = 0.295$ ) for the 2D triangular lattice with NN and NNN exchange interaction, and  $c_p \approx 0.5$  for stage-2

$\text{Co}_c\text{Mg}_{1-c}\text{Cl}_2$  GIC, which is close to the theoretical value ( $c_p = 0.5$ ) for the 2D triangular lattice with NN exchange interaction. It is found from the comparison between the magnetic phase diagrams of  $\text{Co}_c\text{Mg}_{1-c}\text{Cl}_2$  and stage-2  $\text{Co}_c\text{Mg}_{1-c}\text{Cl}_2$  GIC that (i) the effect of the dimensionality on the dilution with Mg ions becomes important below  $c \approx 0.7$ , and that (ii) the effect of the NNN interaction on the dilution with Mg ions becomes significant below  $c \approx 0.5$ . In  $\text{Co}_c\text{Mg}_{1-c}\text{Cl}_2$  there may be a possibility of a spin-glass phase arising from the competition between ferromagnetic NN exchange interaction and antiferromagnetic NNN exchange interaction. We find that the peak susceptibility of  $\text{Co}_c\text{Mg}_{1-c}\text{Cl}_2$  increases with decreasing Co concentration. This increase of peak susceptibility near the percolation threshold may be attributed to either the paramagnetic susceptibility arising from isolated magnetic ions or the destruction of the balance of the two antiferromagnetic sublattices by nonmagnetic atoms.

In conclusion, the pristine  $\text{Co}_c\text{Mg}_{1-c}\text{Cl}_2$  and stage-2  $\text{Co}_c\text{Mg}_{1-c}\text{Cl}_2$  GIC provide model systems for studying the magnetic phase transitions of site-diluted 3D  $XY$  and 2D  $XY$  spin systems. Through the present work we understand the role of the dimensionality on the magnetic phase transitions of random spin systems. A better understanding of the percolation problem would be possible by measurements such as heat capacity and neutron scattering.

## ACKNOWLEDGMENTS

We would like to thank Hiroyoshi Suematsu for providing us with high-quality single-crystal kish graphites. We are grateful to Michael Kellicutt and William Brinkman for their help on the dc and ac magnetic susceptibility measurements. This work was supported by NSF Grant No. DMR-8902351.

- <sup>1</sup>M. Suzuki, *CRC Crit. Rev. Solid State Mater. Sci.* **16**, 237 (1990).
- <sup>2</sup>G. Dresselhaus, J. T. Nicholls, and M. S. Dresselhaus, in *Graphite Intercalation Compounds II*, edited by H. Zabel and S. A. Solin (Springer-Verlag, Berlin, 1992).
- <sup>3</sup>M. Yeh, I. S. Suzuki, M. Suzuki, and C. R. Burr, *J. Phys. Condens. Matter* **2**, 9821 (1990).
- <sup>4</sup>I. S. Suzuki, M. Suzuki, L. F. Tien, and C. R. Burr, *Phys. Rev. B* **43**, 6393 (1991).
- <sup>5</sup>I. S. Suzuki, F. Khemai, M. Suzuki, and C. R. Burr, *Phys. Rev. B* **45**, 4721 (1992).
- <sup>6</sup>J. T. Nicholls and G. Dresselhaus, *Phys. Rev. B* **41**, 9744 (1990).
- <sup>7</sup>K. Katsumata, S. Kawai, and J. Tuchendler, *Solid State Commun.* **65**, 1211 (1988).
- <sup>8</sup>F. Hulliger, in *Structural Chemistry of Layer-Type Phases*, edited by F. Lévy (Reidel, Dordrecht, 1976).
- <sup>9</sup>A. F. Wells, *Structural Inorganic Chemistry* (Clarendon, Oxford, 1983).
- <sup>10</sup>M. E. Lines, *Phys. Rev.* **131**, 546 (1963).
- <sup>11</sup>M. T. Hutchings, *J. Phys. C* **6**, 3143 (1973).
- <sup>12</sup>D. G. Wiesler, M. Suzuki, P. C. Chow, and H. Zabel, *Phys. Rev. B* **34**, 7951 (1986).
- <sup>13</sup>D. G. Wiesler, M. Suzuki, and H. Zabel, *Phys. Rev. B* **36**, 7051 (1987).
- <sup>14</sup>M. K. Wilkinson, J. W. Cable, E. O. Wollan, and W. C. Koehler, *Phys. Rev.* **113**, 497 (1959).
- <sup>15</sup>C. Starr, F. Bitter, and A. R. Kaufmann, *Phys. Rev.* **58**, 977 (1940).
- <sup>16</sup>D. Bertrand, F. Bensamka, A. R. Fert, J. Gelard, J. P. Redoules, and S. Legrand, *J. Phys. C* **17**, 1725 (1984).
- <sup>17</sup>W. Y. Ching and D. L. Huber, *Phys. Rev. B* **13**, 2962 (1976).
- <sup>18</sup>R. B. Stinchcombe, in *Phase Transitions and Critical Phenomena*, edited by C. Domb and J. L. Lebowitz (Academic, New York, 1983), Vol. 7, p. 151.
- <sup>19</sup>S. A. Solin and H. Zabel, *Adv. Phys.* **37**, 87 (1988).
- <sup>20</sup>I. S. Suzuki and M. Suzuki, *J. Phys. Condens. Matter* **3**, 8825 (1991).
- <sup>21</sup>L. J. de Jongh and A. R. Miedema, *Adv. Phys.* **23**, 1 (1974).
- <sup>22</sup>Y. Okuda, I. Yamada, J. Watanabe, and T. Haseda, *J. Phys. Soc. Jpn.* **49**, 2136 (1980).
- <sup>23</sup>D. J. Breed, K. Gilijamse, J. W. E. Sterkenburg, and A. R.

- Miedema, *Physica* **68**, 303 (1973).
- <sup>24</sup>T. Enoki and I. Tsujikawa, *J. Phys. Soc. Jpn.* **39**, 324 (1975).
- <sup>25</sup>A. B. Harris and S. Kirkpatrick, *Phys. Rev. B* **16**, 542 (1977).
- <sup>26</sup>D. Stauffer, *Z. Phys. B* **22**, 161 (1976).
- <sup>27</sup>H. E. Stanley, R. J. Birgeneau, P. J. Reynolds, and J. E. Nicoll, *J. Phys. C* **9**, L553 (1976).
- <sup>28</sup>T. C. Lubensky, *Phys. Rev. B* **15**, 311 (1977).
- <sup>29</sup>R. A. Cowley, R. J. Birgeneau, G. Shirane, H. J. Guggenheim, and H. Ikeda, *Phys. Rev. B* **21**, 4083 (1980).
- <sup>30</sup>R. A. Cowley, G. Shirane, R. J. Birgeneau, E. C. Svensson, and H. J. Guggenheim, *Phys. Rev. B* **22**, 4412 (1980).
- <sup>31</sup>R. J. Birgeneau, R. A. Cowley, G. Shirane, J. A. Tarvin, and H. J. Guggenheim, *Phys. Rev. B* **21**, 317 (1980).